Available online at www.sciencedirect.com
SCIENCE DIRECT
Optics & Laser Technology 38 (2006) 645–648
Optics & Laser Technology
www.elsevier.com/locate/optlastec

Temperature dependence of the 1.064-μm stimulated emission cross-section of Cr:Nd:YAG crystal

Shengzhi Zhao[a,*], Alexandra Rapaport[b], Jun Dong[b], Bin Chen[b], Peizhen Deng[c], Michael Bass[b]

[a] School of Information Science and Engineering, Shandong University, Jinan 250100, PR China
[b] School of Optics and Center for Research and Education in Optics and Lasers (CREOL), University of Central Florida Orlando, FL 32816-2700, USA
[c] Shanghai Institute of Optics and Fine Mechanics, The Chinese Academy of Science, Shanghai 201800, PR China

Received 30 July 2004; received in revised form 23 December 2004; accepted 24 December 2004
Available online 23 February 2005

Abstract

The fluorescence emission spectra of Cr:Nd:YAG crystal are measured and the effective stimulated emission cross-section of the crystal is obtained from −80 to +80 °C. A linear temperature dependence between −80 and +80 °C is reported for the 1.064-μm peak stimulated emission cross-section of Cr:Nd:YAG crystal.

Keywords: Cr:Nd:YAG crystal; Fluorescence emission spectra; Stimulated emission cross-section; Temperature dependence

1. Introduction

Neodymium-doped crystal of yttrium aluminum garnet (Nd:YAG) is the most commonly used active media for high average power solid state laser applications. Especially, by using Cr, Nd co-doped yttrium aluminum garnet (Cr:Nd:YAG) crystal, the self-Q-switched [1–10] and self-mode-locking Cr:Nd:YAG [11] lasers have been achieved. Generally speaking, optically pumped solid-state lasers using Cr, Nd:YAG may have to operate over a wide range of temperatures. Optical elements in a typical laser resonator (e.g., mirrors, beam splitters, etc.) show no variation of optical properties over a wide range of temperatures. However, the stimulated emission cross-section of the laser transition will depend on temperature and the variation with temperature will affect the lasing performance characteristics, such as threshold, output power, pulse width, etc. The room temperature spectrum properties and stimulated emission cross-section of Nd:YAG crystals have been studied [12,13]. The small-signal gain characteristics of Nd:YAG crystal over the temperature ranges of 250–500 K and the threshold, the slope efficiency of Nd:YAG laser over the temperature ranges of 80–300 K have been given [14,15]. Recently, A. Rapaport presented the temperature dependence of the 1.06-μm stimulated emission cross-section of neodymium in YAG and GSGG crystals [16]. Moreover, Dong studied the temperature-dependent stimulated-emission cross-section and concentration quenching in Nd^{3+}-doped phosphate glasses [17]. However, no systematic study of the variation of the stimulated emission cross-section of Cr, Nd co-doped YAG crystal could be found over the range of temperatures of interest for practical applications. The present paper gives the experimental evidence for a linear temperature dependence of the 1.064-μm peak stimulated emission cross-section of Cr:Nd:YAG crystal between −80 and +80 °C.

*Corresponding author.
E-mail address: shengzhi_zhao@sdu.edu.cn (S. Zhao).

0030-3992/$ - see front matter © 2005 Elsevier Ltd. All rights reserved.
doi:10.1016/j.optlastec.2004.12.012

2. Experiments

The effective stimulated emission cross-section of laser crystal Cr:Nd:YAG at various temperatures can be calculated by recording the entire emission spectrum of the excited crystal and measuring the emission lifetime of the crystal at different temperatures. The experimental setup is shown in Fig. 1. The emission spectra of Cr:Nd:YAG crystal are measured at 850–1500 nm The excitation source is a fiber-coupled diode laser operating at 804 nm and the temperature of diode laser is controlled by an automatic temperature controller. The size of Cr:Nd:YAG crystal with co-doped 0.01 at% Cr and 0.5 at% Nd is 5 mm × 5 mm × 1 mm, and located inside a temperature controller (−80 to +80 °C). Below room temperature, the temperature-controlled compressed helium cryostat is used to cool samples, while above the room temperature, a heating ribbon is wrapped around the sample holder and the temperature is monitored using a calibrated temperature sensor. The light of a diode laser is focused to the Cr:Nd:YAG crystal surface (5 mm × 1.0 mm) with the index gradient lens. The excitation signal is monitored during the experiment with a silicon (Si) detector. The emission fluorescence of the crystal is focused with a lens to Jarell–Ash monochromator. An indium gallium arsenide (InGaAs) detector located at the output slit of the 25 cm focal length monochromator is used to detect the fluorescence emission intensity. With 50-μm slits, the resolution of this detection system is about 0.4 nm.

The experimental arrangement for the emission lifetime measurement is very similar to the above setup for the emission spectrum measurement, except that the excitation source is a tunable optical parametric oscillator (Quanta Ray MOPO-SL, pulse width 5 ns) tuned to 804 nm. In addition, the detection wavelength of Jarell–Ash monochromator is fixed at 1.064 μm and a photo-multiplier tube is connected to the output slit of the monochromator to detect the intensity of the fluorescence emission. The decay curves of the fluorescence are recorded with a storage oscilloscope (TDS694C) and a computer-controlled data acquisition system.

3. Experimental results

The ytterbium emission from Cr:Nd:YAG crystal is not polarization dependent, so the emission spectra obtained could be used to calculate the effective stimulated emission cross-section of an Nd^{3+} ion from the manifold $^4F_{3/2}$–$^4I_{11/2}$ transition in Cr:Nd:YAG by applying the Fuchtbauer–Ladenburg (F–L) formula [18]:

$$\sigma(\lambda) = \frac{1}{8\pi}\frac{\lambda^5\eta}{n^2 c\tau}\frac{I(\lambda)}{\int I(\lambda)\lambda\,\mathrm{d}\lambda}, \quad (1)$$

where λ is the wavelength, $\sigma(\lambda)$ is the effective stimulated emission cross-section at wavelength λ, η is the quantum efficiency (assumed to be close to 1 for Cr:Nd:YAG), n is the index of refraction of the material, c is the speed of light in vacuum, and τ is the fluorescent lifetime of the upper laser level, $I(\lambda)$ is the fluorescent intensity at wavelength λ.

In order to calculate the effective stimulated emission cross-section of crystal with Eq. (1), the fluorescent lifetime τ must be given. For Cr:Nd:YAG crystal at 1.064 μm, from the detected decay curve of the fluorescent intensity at 1.064 μm, the fluorescent lifetime can be obtained with a fit to Forster–Dexter model [19–21]. Fig. 2 is the detected decay curve of the fluorescent intensity at room temperature. A fit to

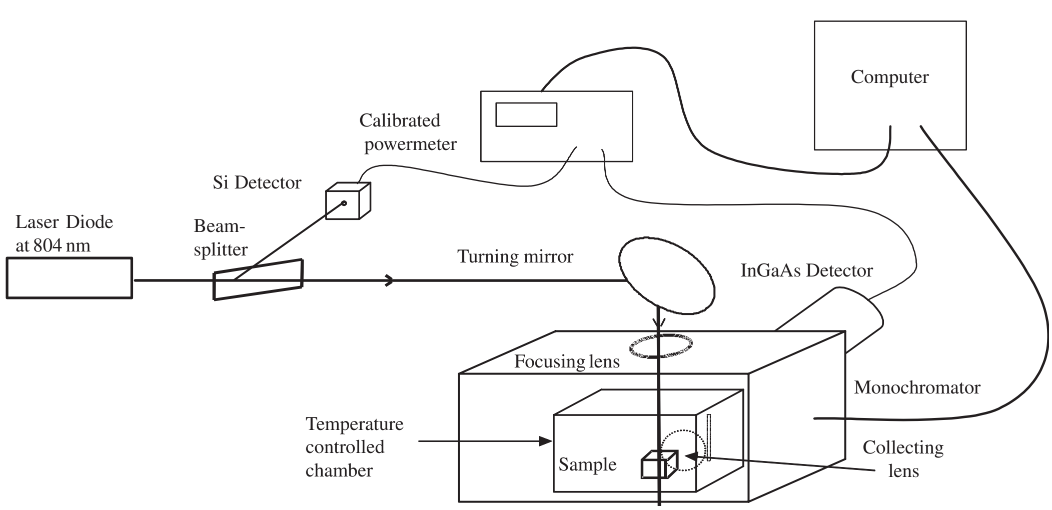

Fig. 1. Experimental setup of fluorescent emission spectrum at different temperature.

Forster–Dexter model shows that the fluorescent lifetime is 220 μs. We measure the fluorescent lifetime of Cr:Nd:YAG crystal at different temperature (from −80 to +80 °C). The results show that the fluorescent lifetime varies little with the temperature at the above temperature ranges. Therefore, we fix its value at 220 μs when evaluating Eq. (1). Similarly, for Cr:Nd:YAG crystal, the index of refraction of the material varies very little over the temperature ranges (−80 to +80 °C), so we use a constant value of 1.82 in Eq. (1).

The fluorescence emission spectrum of Cr:Nd:YAG crystal at room temperature is shown in Fig. 3. According to the $I(\lambda)$ in Fig. 3 and the related parameters, the calculated effective stimulated emission cross-sections by using Eq. (1) are given in Fig. 4. The figure shows that the peak value at 1.064 μm is $2.28 \times 10^{-19}\,\mathrm{cm}^2$.

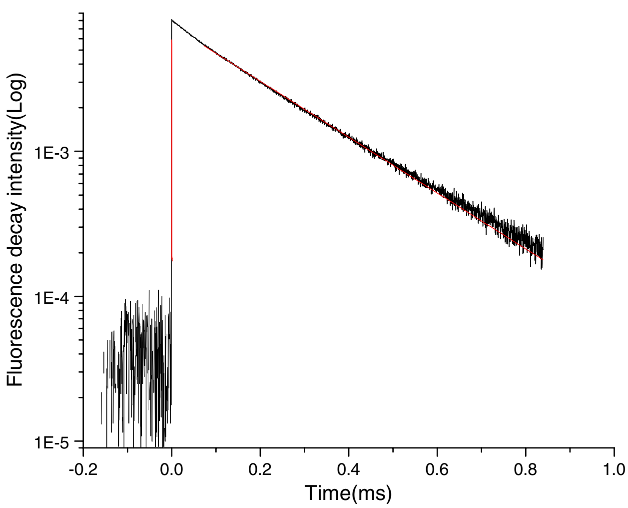

Fig. 2. Fluorescent decay curve of Cr:Nd:YAG crystal at room temperature.

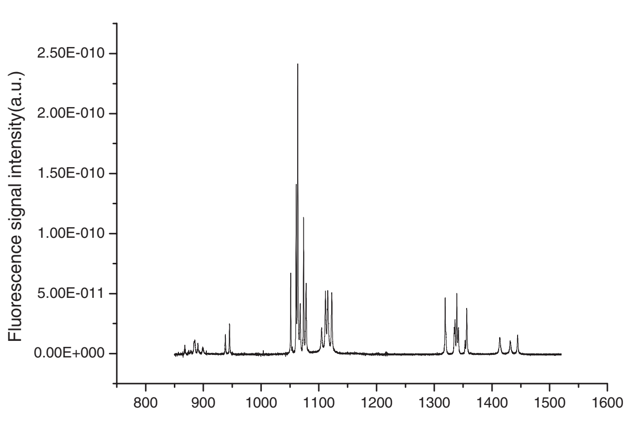

Fig. 3. Fluorescent emission spectrum of Cr:Nd:YAG crystal at room temperature.

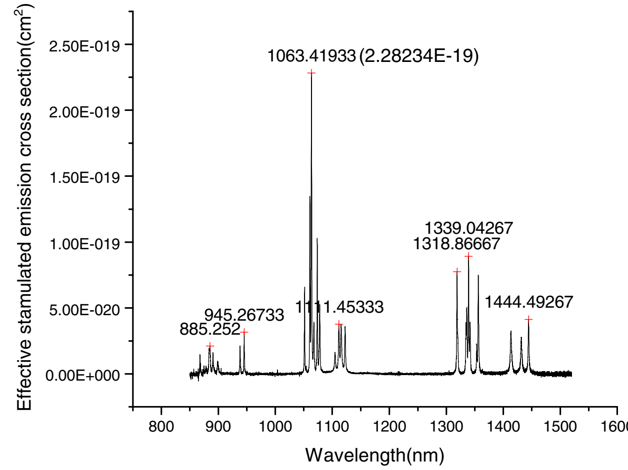

Fig. 4. Effective stimulated emission cross-section of Cr:Nd:YAG crystal at room temperature.

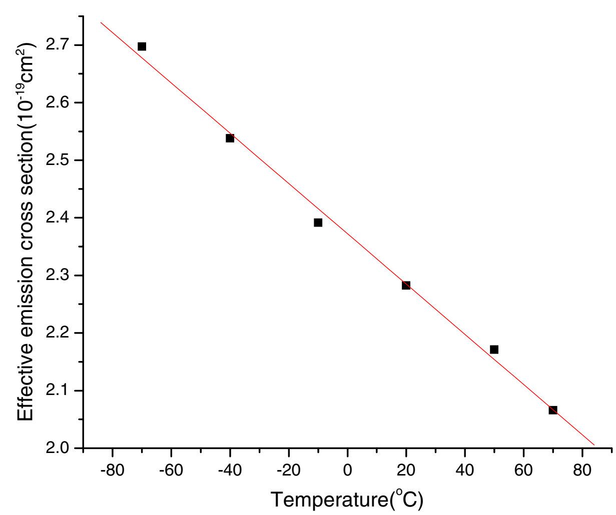

Fig. 5. Effective stimulated emission cross-section versus temperature.

By adjusting the temperature controller system of Cr:Nd:YAG crystal, the fluorescence emission spectra at various temperatures (−80 to +80 °C) can be measured. Using Eq. (1), we can calculate the effective stimulated emission cross-section of Cr:Nd:YAG crystal at 1.064 μm over various temperature ranges. Fig. 5 shows the effective stimulated emission cross-section of Cr:Yb:YAG crystal at 1.064 μm as a function of temperature. The points are the calculated values and the line is a linear fit. The figure shows that the effective stimulated emission cross-section of Cr:Nd:YAG crystal at 1.064 μm varies linearly with temperature with a negative slope of $4.37 \times 10^{-22}\,\mathrm{cm}^2/^{\circ}\mathrm{C}$. If T stands for temperature in °C, the effective stimulated emission cross-section σ (cm^2) can be expressed as

$$\sigma = (2.32 - 4.37 \times 10^{-2}\,\mathrm{T}) \times 10^{-20}. \quad (2)$$

4. Conclusion

The fluorescent emission spectra and radiative lifetime of Cr:Nd:YAG crystal from −80 to +80 °C are measured and the peak stimulated emission cross-section at 1.064 μm for different temperatures are calculated. A linear temperature dependence between −80 and +80 °C is given for the peak stimulated emission cross-section of Cr^{3+} ions and Nd^{3+} ions co-doped YAG.

Acknowledgments

This work is supported by the Science and Technology Development Program of Shandong Province.

References

[1] Zhou S, Lee KK, Chen YC. Monolithic self-Q-switched Cr, Nd:YAG laser. Opt Lett 1993;18:511–3.
[2] Wang P, Shou-Huan Zhou, Lee KK, Chen YC. Picosecond laser pulse generation in a monolithic self-Q-switched solid state laser. Opt Commun 1995;114:439–41.
[3] Liu H, Hornia O, Chen YC, Zhou S. Single-frequency Q-switched Cr, Nd:YAG laser operating at 946-nm wavelength. IEEE J Selected Topics Quantum Electron 1997;3:26–8.
[4] Liu H, Zhou S, Chen YC. High-power monolithic unstable-resonator solid-state laser. Opt Lett 1998;23:451–5.
[5] Dong J, Deng P, et al. Laser-diode-pumped Cr^{4+}, Nd^{3+}:YAG with self-Q-switched laser output of 1.4 W. Opt Lett 2000; 25:1101–3.
[6] Lanbin Lv, Ling W, et al. Diode-pumped self-Q-switched single-frequency 946-nm Nd^{3+}, Cr^{4+}:YAG microchip laser. Opt Lett 2001;26:72–4.
[7] Li D-H, Wang L, et al. Intracavity-doubled self-Q-switched Nd, Cr:YAG 946/473 nm microchip laser. Chin Phys Lett 2002; 19:504–7.
[8] Dong J, Deng P, Mass M. Cr, Nd:YAG self-Q-switched laser with high efficiency output. Opt Laser Technol 2002;34:589–94.
[9] Dong J, Deng P. Laser performance of monolithic Cr, Nd:YAG self-Q-switched laser. Opt Commun 2003;220:425–31.
[10] Kalisky Y, Kravchik L, et al. Performance of diode-end-pumped Cr^{4+}, Nd^{3+}:YAG self-Q-switched and Nd:YAG/Cr^{4+}:YAG diffusion bonded lasers. Opt Mater 2004;24:607–14.
[11] Yang L, Feng B-H, et al. Self-mode-locking in a diode-pumped self-Q-switched Nd^{3+}, Cr^{4+}:YAG laser. Chin Phys Lett 2002;19: 1450–3.
[12] Singh S, Smith RG, Van Uiter LG. Stimulated emission cross section and fluorescent quantum efficiency of Nd in yttrium aluminum garnet at room temperature. Phys Rev B 1974;10: 2566–72.
[13] Kushida T, Marcos HM, Geusic JE. Laser transition cross-section and fluorescent branching ratio for Nd^{3+} in yttrium aluminum garnet. Phys Rev 1968;167:289–91.
[14] Buchenkov VA, Vitrishchak IB, Evdokimova VG, Soms LN, Stepanov AI, Stupnikov VK. Temperature dependence of giant pulse amplification in Nd^{3+}:YAG. Sov J Quantum Electron 1981; 11:702–5.
[15] Brauch U, Muckenschnabel J. Temperature dependence of flashlamp-pumped Nd:YAG and Nd:Cr:GSGG lasers. Opt Commun 1989;73(1):62–6.
[16] Rapaport A, Zhao S, et al. Temperature dependence of the 1.06-μm stimulated emission cross section of neodymium in YAG and GSGG. Appl Opt 2002;41:7052–7.
[17] Dong J, Bass M, et al. Temperature-dependent stimulated-emission cross section and concentration quenching in Nd^{3+}-doped phosphate glasses. J Opt Soc Am B 2004;21:454–7.
[18] Moulton PE. Spectroscopic and laser characteristics of Ti:Al_2O_3. J Opt Soc Am B 1986;3:125–33.
[19] Forster T. Transfer mechanisms of electronic excitation energy. Radiat Res Suppl 1960;2:326–39.
[20] Dexter DL. A theory of sensitized luminescence in solids. J Chem Phys 1953;21:836–50.
[21] Sakun VP. Kinetics of energy transfer in a crystal. Sov Phys Solid State 1973;14:1906–14.